Intramolecular Quenching of Excited Singlet States by Stable Nitroxyl Radicals

S. A. Green,[†] D. J. Simpson,[†,§] G. Zhou,[‡] P. S. Ho,[‡] and N. V. Blough*,[†]

Contribution from the Department of Chemistry, Woods Hole Oceanographic Institution, Woods Hole, Massachusetts 02543, and Department of Biochemistry and Biophysics, Oregon State University, Corvalis, Oregon 97331. *Received March 15, 1990*

Abstract: Absorbance and steady-state and time-resolved fluorescence measurements were employed to examine the mechanism(s) of excited singlet state quenching by nitroxides in a series of nitroxide–fluorophore adducts. This work establishes the following: (1) the absorption and emission energies of the fluorophores are unaffected by the presence of the nitroxide substituent(s), and the residual emission that is observed from the adducts arises from the locally excited singlet of the fluorophore, not from charge recombination; (2) rate constants for intramolecular quenching by the nitroxides (k_q) are high (10^8–10^{10} s^{-1}) and decrease significantly with increasing nitroxide to fluorophore distance—however, relatively high rates of quenching ($>10^8$ s^{-1}) are observed over distances as great as 12 Å; (3) Förster energy transfer does not contribute significantly to the quenching due to the low values for the spectral overlap integrals; (4) the k_q's do not increase proportionally to the solvent-dependent increases in the Dexter overlap integral, indicating that energy transfer by the Dexter mechanism is not responsible for the quenching; (5) the values of k_q show no obvious correlation with the calculated free energies for photoinduced electron transfer, suggesting that this quenching pathway is also unimportant; (6) for hematoporphyrin–nitroxide adducts, which contain a fluorophore whose singlet energy is below that of the first excited state energy of the nitroxide (thus precluding energy transfer), significant rates of quenching are still observed; (7) for compounds with similar nitroxide–fluorophore distance, an approximately linear correlation is observed between the k_q's of the paramagnetic compounds and the nonradiative rate constants of the diamagnetic reference compounds, suggesting that the nitroxide moiety catalyses a preexisting nonradiative pathway in the fluorophore. These results indicate that the quenching arises through electron exchange which causes relaxation of the (local) singlet state to the triplet and/or ground state of the fluorophore.

Introduction

Diffusional quenching by stable nitroxyl radicals of excited singlet,[1] doublet,[2] and triplet[1d,f,3-10] states and of excimers[11] has been studied extensively over the past 20 years. The goal of much of this work has been to understand the mechanism(s) through which excited states are quenched by paramagnetic species. Recently however, fluorescence quenching by nitroxides has also become an important tool with which to probe the structural and dynamical properties of membranes[12] and micelles.[13]

While it has been generally accepted that nitroxide quenching of singlet states can result from an electron exchange-induced[14] intersystem crossing to the triplet[1b,e] or internal conversion to the ground state,[1e-g] significant contributions to the quenching may also arise from charge[1f] and/or energy transfer.[1a,12d] Green et al.[1b] argued that charge (electron) transfer is unimportant owing to a lack of solvent dependence of the quenching rate constant. However, as noted by Chattopadhyay et al.,[1f] the quenching occurs at the diffusion limit and thus may not be differentiated by solvent polarity.[15] Green et al.[1b] also suggested that Förster energy transfer[16] is insignificant because of the low extinction coefficients of the nitroxides in the 400–550 nm spectral region. Recent work by Puskin et al.[12d] suggests that energy transfer can be important and, in some cases, can extend the quenching radius to as much as 10 Å, approximately twice the interaction distance originally calculated by Green et al.[1b] Furthermore, energy transfer by electron exchange[17] cannot be excluded a priori for compounds having singlet energies greater than the lowest excited state energy of the nitroxide (~2.6 eV for the piperidinyl nitroxides).

Until recently, information on the efficiency of intramolecular quenching of excited states by nitroxide was unavailable. We have shown that intramolecular quenching of excited singlets is highly efficient[18] and that covalently linked, nitroxide-fluorophore adducts can be employed as very sensitive optical probes of radical/redox reactions.[18-21] These adducts also offer a means of studying the mechanism(s) of nitroxide quenching in more detail and of establishing the distance dependence and possible importance of "through-bond"[15] vs "through-space" interactions in the quenching. This information is essential for the construction of better optical

* To whom correspondence should be addressed.
† Woods Hole Oceanographic Institution.
‡ Oregon State University.
§ Present address: Life Sciences Division, Los Alamos National Laboratory, Los Alamos, NM 87545.

(1) (a) Buchachenko, A. L.; Khloplyankina, M. S.; Dobryakov, S. N. *Opt. Specktrosk.* (USSR) **1967**, *22*, 554–556. (b) Green, J. A.; Singer, L. A.; Parks, J. H. *J. Chem. Phys.* **1973**, *58*, 2690–2695. (c) Darmanyan, A. P.; Tatikolov, A. S. *J. Photochem.* **1986**, *32*, 157–163. (d) Watkins, A. R. *Chem. Phys. Lett.* **1974**, *29*, 526–528. (e) Kuzmin, V. A.; Tatikolov, A. S. *Chem. Phys. Lett.* **1977**, *51*, 45. (f) Chattopadhyay, S. K.; Das, P. K.; Hug, G. L. *J. Am. Chem. Soc.* **1983**, *105*, 6205–6210. (g) Yee, W. A.; Kuzmin, V. A.; Kliger, D. S.; Hammond, G. S.; Twarowski, A. J. *J. Am. Chem. Soc.* **1979**, *101*, 5104.

(2) Samanta, A.; Bhattacharyya, K.; Das, P. K.; Kamat, P. V.; Weir, D.; Hug, G. L. *J. Phys. Chem.* **1989**, *93*, 3651.

(3) (a) Singer, L. A.; Davis, G. A. *J. Am. Chem. Soc.* **1967**, *89*, 158. (b) Singer, L. A.; Davis, G. A.; Muralidharan, V. P. *J. Am. Chem. Soc.* **1969**, *91*, 897.

(4) (a) Yang, N. C.; Loeschen, R.; Mitchell, D. *J. Am. Chem. Soc.* **1967**, *89*, 5465. (b) Chapman, O. L.; Koch, T. H.; Klein, F.; Nelson, P. J.; Brown, E. L. *J. Am. Chem. Soc.* **1968**, *90*, 1657.

(5) (a) Schwerzel, R. E.; Caldwell, R. A. *J. Am. Chem. Soc.* **1973**, *95*, 1382. (b) Caldwell, R. A.; Schwerzel, R. E. *J. Am. Chem. Soc.* **1972**, *94*, 1035–1037.

(6) Gijzeman, O. L. J.; Kaufman, F.; Porter, G. *J. Chem. Soc., Faraday Trans. 2* **1973**, *69*, 727–737.

(7) Watkins, A. R. *Chem. Phys. Lett.* **1980**, *70*, 262.

(8) (a) Kuzmin, V. A.; Tatikolov, A. S.; Borisevich, Y. E. *Chem. Phys. Lett.* **1978**, *53*, 52. (b) Kuzmin, V. A.; Tatikolov, A. S. *Chem. Phys. Lett.* **1978**, *53*, 606. (c) Borisevich, Y. E.; Kuzmin, V. A.; Renge, I. V.; Darmanyan, A. P. *Izv. Akad. Nauk. SSSR Ser. Khim.* **1981**, *9*, 2014. (d) Borisevich, Y. E.; Kuzmin, V. A.; Kokorin, A. I.; Sennikov, G. P.; Novozhilova, G. A.; Shapiro, A. B. *Izv. Akad. Nauk. SSSR Ser. Khim.* **1981**, *9*, 2019.

(9) Kuzmin, V. A.; Kliger, D. S.; Hammond, G. S. *Photochem. Photobiol.* **1980**, *31*, 607.

(10) Chattopadhyay, S. K.; Kumar, C. V.; Das, P. K. *J. Photochem.* **1985**, *30*, 81.

(11) Green, J. A.; Singer, L. A. *J. Am. Chem. Soc.* **1974**, *96*, 2730.

(12) (a) London, E. *Mol. Cell. Biochem.* **1982**, *45*, 181 and references cited therein. (b) Chattopadhyay, A.; London, E. *Biochemistry* **1987**, *26*, 39. (c) Winiski, A. P.; Eisenberg, M.; Langner, M.; McLaughlin, S. *Biochemistry* **1988**, *27*, 386. (d) Puskin, J. S.; Vistnes, A. I.; Coene, M. T. *Arch. Biochem. Biophys.* **1981**, *206*, 164.

(13) (a) Atik, S. S.; Singer, L. A. *J. Am. Chem. Soc.* **1978**, *100*, 3234. (b) Atik, S. S.; Kwan, C. L.; Singer, L. A. *J. Am. Chem. Soc.* **1979**, *101*, 5696. (c) Atik, S. S.; Singer, L. A. *Chem. Phys. Lett.* **1978**, *59*, 519. (d) Scaiano, J. C.; Paraskevopoulos, C. I. *Can. J. Chem.* **1984**, *62*, 2351.

(14) (a) Hoytink, G. J. *Acc. Chem. Res.* **1969**, *2*, 114. (b) Birks, J. B. *Photophysics of Aromatic Molecules*; Wiley-Interscience: London, 1970; pp 492–517. (c) Turro, N. J. *Modern Molecular Photochemistry*, Benjamin-Cummings Pub. Co. Inc.: Menlo Park, CA, 1978; Chapter 6.

0002-7863/90/1512-7337$02.50/0

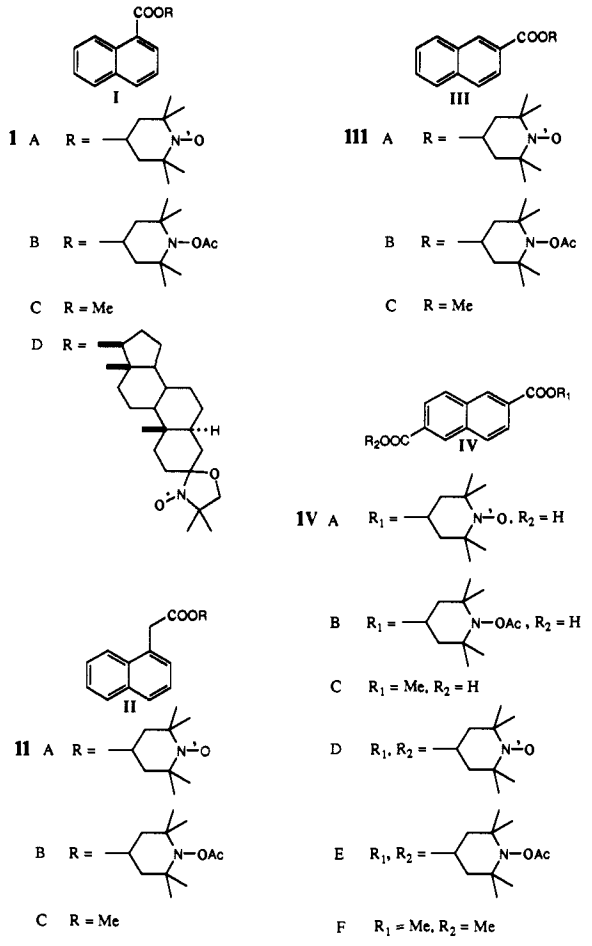

Figure 1. Naphthalene derivatives examined in this study.

radical sensors,[18-20] for a more complete analysis of nitroxide quenching in biophysical studies,[12,13] and for an understanding of the possible influence of stable or transient radicals on excited states in biological and chemical systems.

In this study, we examine the photophysical properties of a number of nitroxide–fluorophore adducts and their diamagnetic analogues. By employing compounds having fluorophores with differing singlet energies and a range of nitroxide-fluorophore distances, we attempt to assess the relative contributions of energy transfer, electron transfer, and electron exchange induced relaxation to the intramolecular quenching of singlet states by nitroxides.

Results and Discussion

A. Absorption, Excitation, and Emission Spectra. Table I summarizes the absorption and emission energies of I–IV (Figure 1) in various solvents. In water, methanol, acetonitrile, dioxane, and hexane, the absorption spectra of the nitroxide–fluorophore adducts were indistinguishable from the sum of the individual spectral contributions of the fluorophore and nitroxide substituents. Other than the loss of the weak nitroxide contribution in the visible (430–480 nm, $\epsilon \approx 10$–$13\ M^{-1}\ cm^{-1}$) and ultraviolet ($\sim$246 nm, $\epsilon \approx 2 \times 10^3\ M^{-1}\ cm^{-1}$), the spectra of the *O*-acetyl and methyl ester derivatives (Figure 1) were identical with those of the corresponding nitroxides. No evidence for optical charge transfer bands or enhanced ground to triplet absorption[14] by the fluorophore could be found in the spectra of the nitroxide adducts. While the absorption spectra of the fluorophores were largely insensitive to solvent polarity, the lowest energy band ($n-\pi^*$) of the nitroxides[22] shifted substantially to the blue with increasing solvent polarity as previously noted.[23] The influence of this shift on singlet state quenching will be addressed below (section D).

The fluorescence excitation spectra of the nitroxide adducts matched the absorption spectra of the fluorophore substituents and were indistinguishable from the excitation spectra of the corresponding diamagnetic derivatives.

The line shapes of the emission spectra were identical for the nitroxide adducts and the corresponding diamagnetic derivatives and generally showed a mirror-image relationship to the excitation spectra (Figure 2). With increasing solvent polarity, identical red shifts in the emission maxima were observed for the nitroxide

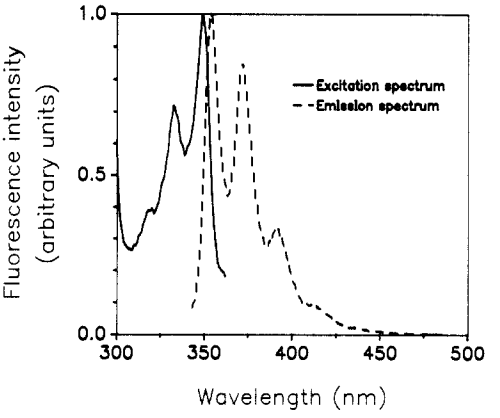

Figure 2. Fluorescence excitation and emission spectra of IVD in hexane.

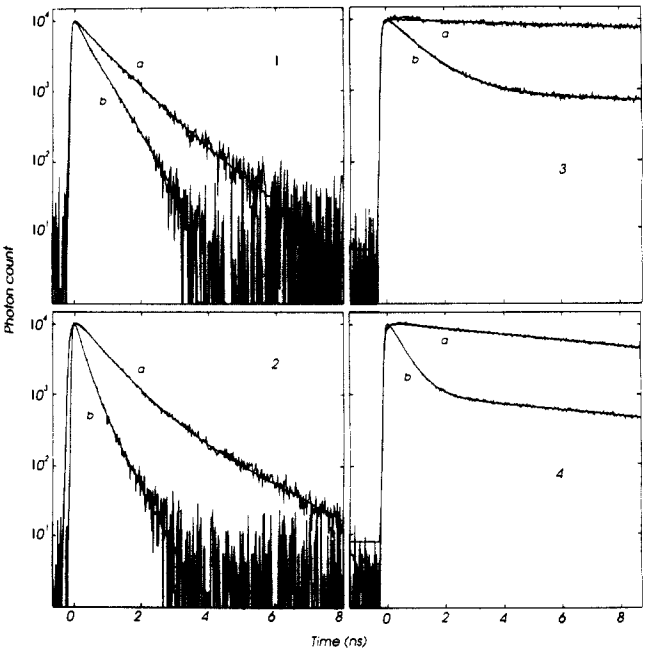

Figure 3. Fluorescence decays of nitroxide adducts (b) as compared to diamagnetic analogues (a): (1) ID and IB in acetonitrile: (2) ID and IB in hexane; (3) IIA and IIB in acetonitrile; and (4) IIIA and IIIB in acetonitrile. Excitation wavelength was 295 nm. Emission was monitored at the peak maximum for each compound (see Table I).

(15) (a) Closs, G. L.; Calcaterra, L. T.; Green, N. J.; Penfield, K. W.; Miller, J. R. *J. Phys. Chem.* **1986**, *90*, 3673. (b) Oevering, H.; Verhoeven, J. W.; Paddon-Row, M. N.; Cotsaris, E.; Hush, N. S. *Chem. Phys. Lett.* **1988**, *143*, 488. (c) Kroon, J.; Oliver, A. M.; Paddon-Row, M. N.; Verhoeven, J. W. *J. Am. Chem. Soc.* **1990**, *112*, 4868.
(16) Förster, T. *Ann. Phys. (Leipzig)* **1948**, *2*, 55.
(17) Dexter, D. L. *J. Chem. Phys.* **1953**, *21*, 836.
(18) Blough, N. V.; Simpson, D. J. *J. Am. Chem. Soc.* **1988**, *110*, 1915.
(19) (a) Kieber, D. J.; Blough, N. V. *Anal. Chem.*, in press. (b) Kieber, D. J.; Blough, N. V. *Free Radical Res. Commun.* **1990**, *10*, 109.
(20) Gerlock, J. L.; Zacmanidis, P. J.; Bauer, D. R.; Simpson, D. J.; Blough, N. V.; Salmeen, I. T. *Free Radical Res. Commun.* **1990**, *10*, 119.
(21) Blough, N. V. *Environ. Sci. Technol.* **1988**, *22*, 77.
(22) (a) Kikuchi, O. *Bull. Chem. Soc. Jpn.* **1969**, *42*, 47. (b) Salotto, A. W.; Burnelle, L. *J. Chem. Phys.* **1970**, *53*, 333.
(23) (a) Briere, R.; Lemaire, H.; Rassat, A. *Bull. Soc. Chim. Fr.* **1965**, 3273. (b) Mukerjee, P.; Ramachandran, C.; Pyter, R. A. *J. Phys. Chem.* **1982**, *86*, 3189–3197.

Table I. Absorption and Fluorescence Maxima of I–IV[a]

compd	absorbance in methanol		fluorescence emission maxima, nm			
	abs max, nm	ϵ, M^{-1} cm^{-1}	hexane	acetonitrile	methanol	water
series I	222	4.2×10^4	332	361	369	390
	300	7.1×10^3	343			
			358			
series II[b]	228		328	326	326	325
	274		340	335	337	335
	284		318	353		
	294		352	371		
series III	242	1.9×10^4 (8.9×10^4)	336	344	364	376
	276	7.9×10^3	352	359	351	
	284	9.6×10^3 (1.3×10^4)	367	375		
	296	6.8×10^3 (9.7×10^3)	388			
	324	1.6×10^3 (2.2×10^3)				
	338	1.9×10^3 (2.7×10^3)				
series IVA–C	248	7.0×10^4	355	359	359	360
	288	1.2×10^4	373	377	374	381
	298	1.1×10^4	393	397	396	
	334	1.8×10^3	416	426		
	348	2.0×10^3				
series IVD–F	246	8.3×10^4 (8.4×10^4)	354	360	363	
	286	1.4×10^4	372	378	380	
	296	1.4×10^4 (1.3×10^4)	391	400		
	338	2.1×10^3 (2.3×10^3)		425		
	352	2.4×10^3 (2.8×10^3)				

[a] Absorption spectra and extinction coefficients measured in methanol. Values in parentheses are extinction coefficients for methyl esters (IIIC and IVF) for which the coefficient differs slightly from that of the nitroxide derivative. The nitroxide contributions to the absorption of I–IVA and I,IVD are described in the text and Figure 4. [b] Series II compounds were isolated as oils; extinction coefficients were not measured.

Table II. Fluorescence Lifetimes and Quantum Yileds of I–IV[a]

	hexane		acetonitrile		methanol[b]		water[c]	
	τ, ns	ϕ	τ, ns	ϕ	τ, ns	ϕ	τ, ns	ϕ
Series I								
A	(0.021)[d]	0.002	(0.033)[d]	0.004	(0.054)[d]	0.006	0.10	0.013 (0.009)[d]
B	0.73	0.05	1.7	0.22	2.8	0.31	7.1	0.66
C	1.00	0.06	1.8	0.20	2.9	0.28	7.3	0.57
D	0.48	0.03	1.1	0.14	1.1	0.12	–	–
Series II								
A	1.09	0.004 (0.006)	1.1	0.006 (0.004)	0.81	0.013 (0.004)	0.40	0.008 (0.002)
B	37.0	0.22	33.7	0.13	43.1	0.20	28.3	0.17
C	49.2	0.22		0.16	43.3	0.21		0.17
Series III								
A	0.52	0.017 (0.019)	0.50	0.016 (0.011)	0.65	0.026 (0.019)	0.46	0.031 (0.012)
B	9.0	0.33	12.4	0.28	11.0	0.32	10.9	0.28
C	9.8	0.38		0.30	11.0	0.30		0.32
Series IV								
A	0.29	0.009 (0.008)	0.33	0.013 (0.012)	0.54	0.010 (0.014)	0.70	0.029 (0.016)
B	14.1	0.40	13.2	0.52	1.1	0.028	12.2	0.28
C	11.5	0.48	13.7		1.2	0.046	12.3	
D	0.21	0.005 (0.006)	0.22	0.006 (0.007)	0.27	0.008 (0.009)	–	–
D	15.3	0.46	13.8	0.46	13.9	0.45	–	–
F	16.1	0.54	15.0	0.50	14.1	0.40	–	–

[a] Values in parentheses were calculated from eq 3. [b] Values in methanol are ~30% lower than those previously reported[18] due to correction of undocumented normalization and conversion routines in the SLM-Aminco software. [c] "Water" measurements for IVA–C were done in pH 8, 50 mM phosphate buffer; ID and IVD–F are not water soluble. [d] Calculated lifetimes only are reported for IA, except in water, because they were below the time resolution of the instrument. Values were calculated from quantum yields of IA and lifetimes of IB by using eq 3.

and diamagnetic adducts of a given substitution. These results indicate that the residual emission from the nitroxide adducts is arising from the same locally excited singlet state of the fluorophore substituent as in the diamagnetic derivatives and is not produced through charge recombination.[24] No evidence for exciplex emission from the paramagnetic adducts could be found in either polar (acetonitrile) or nonpolar (hexane) solvents.

B. Quantum Yield and Lifetime Measurements. While the presence of the nitroxyl radical substituent(s) did not influence the absorption and emission energies of the fluorophores in the adducts, the fluorescence quantum yields and lifetimes of the nitroxide adducts were reduced substantially relative to their corresponding diamagnetic derivatives in both polar and nonpolar solvents (Table II, Figure 3). The fluorescence decay of the nitroxide adducts could be well-fit to a sum of two exponentials but was dominated by the short-lived component (Figure 3). The small, long-lived component usually represented ≤5% of the total amplitude. We attribute this component to minor diamagnetic contaminants, on the basis of assessments of compound purity.

With few exceptions, the fluorescence decay of the diamagnetic derivatives could be fit as a single exponential process (Figure 3). The *O*-acetyl and methyl ester derivatives of a given substitution showed very similar lifetimes and quantum yields (Table II). These results indicate that the rate constants for radiative and nonradiative decay of the singlet do not differ significantly between the *O*-acetyl and the methyl ester derivatives (Figure 1). This leads us to conclude that, unlike the situation for aliphatic and aromatic amines,[25] intramolecular quenching (via electron

(24) Kosower, E. M.; Huppert, D. *Ann. Rev. Phys. Chem.* **1986**, *37*, 127.

(25) Davidson, R. S. *Adv. Phys. Org. Chem.* **1983**, *19*, 1a.

Table III. Rate Constants for Intramolecular Quenching in the Naphthalene–Nitroxide Adducts[a]

compd	$k_q \times 10^{-9}$ s^{-1} hexane	acetonitrile	methanol	water
IA	45	30	18	9.7
ID	0.7 ± 0.3	0.3 ± 0.1	0.5 ± 0.1	–
IIA	0.9	0.9	1.2	2.5
IIIA	1.8	1.9	1.4 ± 0.2	2.1
IVA	3.4	3.0	0.9	1.3
IVD	4.7	4.5 ± 0.5	3.7 ± 0.4	–

[a] Rate constants were calculated from fluorescence lifetimes (or quantum yields, in the case of compound IA, see Table II) by using eq 4. Uncertainties are ±10% except where otherwise noted.

transfer) by the hindered, O-substituted hydroxylamines is unimportant. Preliminary work on other O-substituted hydroxylamines is consistent with this conclusion.[19] In contrast, the unsubstituted hydroxylamine does appear to quench partially.[19,26]

The steady-state and time-resolved fluorescence measurements of the paramagnetic and diamagnetic forms can be related by

$$\phi_d = \frac{k_r}{k_r + k_{nr}} \qquad k_r + k_{nr} = \frac{1}{\tau_d} \tag{1}$$

$$\phi_p = \frac{k_r}{k_r + k_{nr} + k_q} \qquad k_r + k_{nr} + k_q = \frac{1}{\tau_p} \tag{2}$$

where $\phi_d(\phi_p)$ and $\tau_d(\tau_p)$ are the quantum yields and lifetimes of the diamagnetic (paramagnetic) compounds, respectively, k_r and k_{nr} are the rate constants for radiative and nonradiative decay of the diamagnetic compounds, and k_q is the intramolecular (nonradiative) quenching rate constant attributable to the nitroxide moiety. If k_r and k_{nr} are unaltered by the presence of the nitroxide, then

$$\phi_d/\phi_p = \tau_d/\tau_p \tag{3}$$

$$k_q = 1/\tau_p - 1/\tau_d \tag{4}$$

The measured ratios τ_d/τ_p and ϕ_d/ϕ_p are equal within the uncertainties (Table II), indicating that this condition applies. Errors are largest in the determination of ϕ_p, since traces of highly fluorescent impurities can produce significant overestimates of such low quantum yields, leading to low ϕ_d/ϕ_p ratios. For this reason, rate constants for intramolecular quenching, k_q (Table III) were calculated from the lifetime data employing eq 4, except in the case of compound IA where lifetimes were too short to be resolved by the instrument. For this compound the expected lifetimes were computed from eq 3 with use of the quantum yield data and the lifetime of the diamagnetic *O*-acetyl (IB). Lifetime data show <3% of a long-lived component for IA.[27]

In aprotic solvents such as acetonitrile and hexane, k_q increased from $\approx 10^8$ to 10^{10} s^{-1} in the order ID < IIA < IIIA < IVA < IA. This sequence reflects not only the differences in nitroxide–fluorophore distance but also the type, number and position of the naphthalene–nitroxide linkage(s) (vide infra). With the exception of compounds IA and ID, no significant differences were observed between k_q's measured in polar (acetonitrile) and nonpolar (hexane) solvents. Surprisingly, the k_q's for compounds IA and ID actually increased slightly with decreasing solvent polarity (Table III).

C. Dependence of k_q on Distance, Linkage Position, and Type. Because the distance and orientation of the nitroxide with respect to the fluorophore are not rigidly fixed in these compounds, the molecular mechanics program AMBER[28] was employed to search for the conformations of IA, IIA, and IIIA most likely to exist in solution. The strategy for this search is described in the Experimental Section.

(26) Blough, N. V.; Kieber, D. J. Work in progress.
(27) A long-lived component present at a level of 3% could contribute as many as 50% of the photons to the measured quantum yield. This would result in an *underestimate* of k_q by a factor of 2. Quenching constants reported here, therefore, represent a lower limit for quenching rates in IA.
(28) Weiner, P. K.; Kollmann, P. A. *J. Comput. Chem.* **1981**, *2*, 287.

Table IV. Total Energies, Nitrogen Atom–Naphthalene Ring Distances, and κ^2 for Lowest Energy Conformations of IA, ID, IIA, and IIIA

compd	energy,[a] kcal/mol	distance[b] R, Å	κ^2[c]
IA	22.25	8.24	0.18
	22.30	8.26	0.11
	22.39	8.25	0.12
av[d]	**22.31**	**8.25**	**0.14**
ID[e]		12.2	
IIA	14.64	6.55	0.01
	15.01	7.81	0.03
	15.02	7.41	0.16
	15.18	7.94	0.07
	15.42	8.32	0.21
	15.47	8.66	2.01
	15.54	8.83	0.01
	15.80	7.59	0.17
av[f]	**15.12**	**7.59**	**0.26**
IIIA	16.67	9.04	0.21
	16.68	8.94	0.18
	16.74	9.04	0.33
av[d]	**16.70**	**9.01**	**0.24**

[a] Energy for each conformation is the sum of contributions for bond lengths and angles, and dipole and van der Waals interactions. [b] Distances were measured from the nitrogen atom to the center of the C9–C10 bond of the naphthalene ring. [c] κ^2 was calculated[29] from the emission (naphthalene) and absorption (nitroxide) dipoles. Emission dipoles for 1- and 2-substituted naphthaldehydes (^1L_b transition) were obtained from ref 40. The absorption dipole for the nitroxide group was taken to be perpendicular to the NO bond and lying in the CNC plane, on the basis of the local C_s symmetry of the nitroxide group and the analogy to the $n \rightarrow \pi^*$ transition in carbonyls.[15b,22,23,41] $0 < \kappa^2 < 4$, allowed range. [d] *Numerical* averages of the energies, distances, and κ^2 for the conformations of each compound. [e] Distance for ID was estimated from molecular models by using the same relative orientation of the carbonyl group as that calculated for the lowest energy conformation of IA. [f] Averages for IIA were weighted according to the population in the lowest energy conformation (E = 14.64 kcal/mol) compared with the other seven states (E_{av} = 15.35 kcal/mol). The ratio of population in states 2–8 relative to state 1 is estimated by $N_{(2-8)}/N_{(1)} = g_{(2-8)}/g_{(1)} \times \exp(-\Delta E/RT) = 7 \exp(-(15.35 - 14.64)/RT) = 2.11$.

IA and IIIA were each found to have three unique minimal energy conformations (Table IV). However, the average energy of the low-energy conformations of IIIA was 5.6 kcal/mol lower than that of IA. The higher overall energy of IA can be attributed to a sterically induced distortion of the naphthalene ring and subsequent effects on the dihedral angles within the ring and between the ring and the carboxylate group. This distortion was a result of unfavorable steric interactions between the carbonyl oxygen of the carboxyl group and the hydrogen at position 8 on the naphthalene ring. A rotation of the naphthalene ring by 180° relative to the carboxylate group resulted in greater steric interactions and a more distorted structure. Neither of the other compounds studied displayed this distortion.

In contrast to IA and IIIA, IIA exhibited eight low-energy conformations (Table IV). A single conformer exhibited both the lowest energy and shortest ring to nitrogen distance. Seven other conformers had an average energy that was only 0.7 kcal/mol higher. Because these conformers constituted a large set of thermally accessible states, we were forced to include them in the calculation of average distances. The energies and center-to-center distances of the energetically significant conformations of IA, IIA, and IIIA are summarized in Table IV. Coordinates for each of these conformations are provided in the supplementary material.

The fact that the short-lived fluorescence component of each of these three compounds could be well-fit as a single exponential decay suggests that these conformers interconvert rapidly on the time scale of the quenching (nanoseconds to sub-nanoseconds) or that conformations populated during the lifetime of the singlet do not differ significantly in their ability to quench the singlet state.

The Förster orientation factor, κ^2, was calculated for the conformers of IA–IIIA (Table IV) as a fairly simple means to com-

pare the relative orientations of naphthalene and nitroxide groups. The absence of large variations in κ^2 suggests that differences in the relative orientation of the two groups is probably not the primary factor controlling the variations in quenching rates among these compounds.

The rates of energy transfer (Förster or Dexter) and electron transfer have well-defined distance dependencies. While the rate of Förster energy transfer follows an R^{-6} distance dependence,[16,29] the rates of Dexter transfer and electron transfer are expected to decline exponentially with distance.[15,17,30,31] However, the quenching rates observed in aprotic solvents bear no simple relationship to the nitroxide–naphthalene distances (Tables III and IV), as is illustrated by the following points: (1) while a comparison between IA and ID suggests that increasing R by 4 Å causes k_q to decrease by about 2 orders of magnitude, simply shifting the site of substitution from the α(IA) and β(IIIA) position on the naphthalene ring produces an ~20-fold decrease in k_q, although the values of R for IA and IIIA differ by only 0.76 Å; (2) insertion of a methylene group into the linkage at the α position (IIA) decreases k_q by ~40-fold, although the greater flexibility of this linkage allows a shorter R than either IA or IIIA. As we show below, the rather large variations in k_q observed for compounds having similar nitroxide–naphthalene distances (e.g. IA–IVA) cannot be explained by the differences in the singlet energy of the naphthalenes or by variations in the free energy for photoinduced electron transfer. Instead these variations appear to result from a relationship between k_q and the nonradiative rate constant of the parent (diamagnetic) compound. The presentation and interpretation of this relationship is provided in section D 3.

D. Mechanisms of Quenching. Several mechanisms could contribute to singlet state quenching in these nitroxide adducts. We address here the possible contributions of Förster (dipole–dipole) and Dexter (electron exchange) energy transfer, electron transfer, and electron exchange induced relaxation to the quenching. In principle, k_q reflects the sum of rate constants for each of these potential relaxation pathways

$$k_q = k_{FT} + k_{DT} + k_{ET} + k_{EX} \qquad (5)$$

1. Energy Transfer. In the light of conflicting reports[1a,1b,1f,12d] as to the importance of Förster and Dexter transfer in the quenching of singlet states by nitroxides, we have reexamined this question. Since no emission is observed from the first excited state of the nitroxide, direct spectroscopic evidence for energy transfer was not obtainable. Instead, we compared the observed quenching rates of IA, IIA, and IIIA to the Förster (J_F) and Dexter (J_D) overlap integrals calculated from the fluorescence spectra of IB, IIB, and IIIB and the absorbance spectrum of 4-hydroxy-2,2,6,6-tetramethyl-1-piperdinyloxy (TEMPOL)

$$J_F = \int_0^\infty F(\lambda)\epsilon(\lambda)\lambda^4 d\lambda / \int_0^\infty F(\lambda)d\lambda \qquad (6a)$$

$$J_D = \int_0^\infty F(\lambda)\epsilon(\lambda)d\lambda / \int_0^\infty F(\lambda)d\lambda \int_0^\infty \epsilon(\lambda)d\lambda \qquad (6b)$$

where $F(\lambda)$ is the corrected fluorescence intensity of the fluorophore and $\epsilon_a(\lambda)$ is the extinction coefficient of the acceptor (TEMPOL) at wavelength λ.

The weak nitroxide absorption band overlaps with the red edge of the singlet emission of the naphthyl group. This absorption is solvent dependent[23] (Figure 4), shifting to the blue with increasing solvent polarity and thus increasing the values of J_F and J_D. The degree of spectral overlap is further enhanced in polar solvents for compounds IA and IIIA whose emissions shift to the red with increasing solvent polarity (Table I).

We have used these solvent-dependent changes in the overlap integrals to assess whether the quenching rates vary in the manner

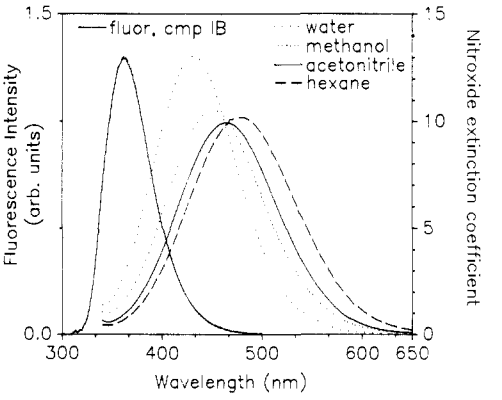

Figure 4. Absorption spectra of TEMPOL in a series of solvents showing the solvent-dependent shifts in the absorption maximum and extinction coefficients (M^{-1} cm^{-1}). Fluorescence emission spectrum of IB in methanol is included in order to illustrate the degree of spectral overlap between naphthalene emission and nitroxide absorption.

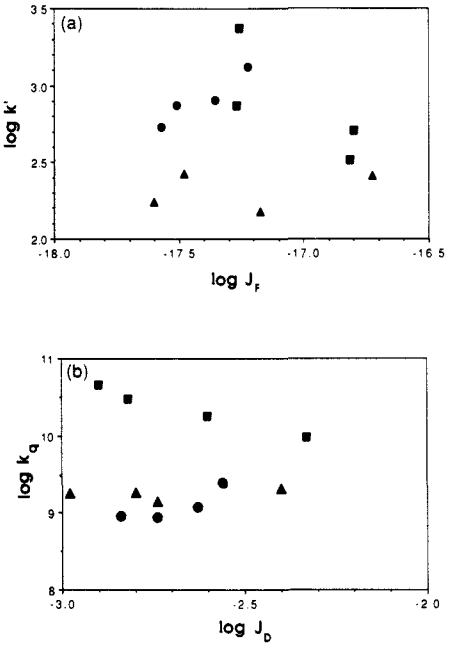

Figure 5. Intramolecular quenching constants vs spectral overlap integrals for IA (■), IIA (▲), and IIIA (●): (a) Förster spectral overlap integral, J_F (M^{-1} cm^3) (the rate constants have been normalized, $k' = k_q \tau d \eta^4 / \phi_d$, to account for solvent dependent variations in lifetime, quantum yield, and refractive index); (b) Dexter spectral overlap J_D (cm).

expected for energy transfer. The rate constant for Förster transfer is given by[29]

$$k_{FT} = \frac{J_F \kappa^2 \phi_d}{R^6 \eta^4 \tau_d} 8.71 \times 10^{23} \qquad (7a)$$

where κ^2 is the orientation factor (Table IV), ϕ_d and τ_p are the quantum yield and lifetime, respectively, of the appropriate diamagnetic *O*-acetyl derivative (Table III), R is the donor–acceptor distance (Table IV), and η is the solvent refractive index.

The rate constant for Dexter transfer is given by[15b]

$$k_{DT} = \frac{4\pi H^2 J_D}{h} = \frac{4\pi^2 H_0^2 e^{-2R/L} J_D}{h} \qquad (7b)$$

where H is the coupling matrix element, H_0 is the preexponential factor, and L is the Bohr radius.

Both of these theories predict that for constant donor–acceptor distance(s) (and orientation(s)) the rate constants for transfer will increase linearly with increasing values of the spectral overlap integrals. However, log plots of k_q vs J_F and J_D for IA, IIA, and IIIA (Figure 5) clearly do not show this relationship (with the possible exception of IIIA in the Förster plot (Figure 5a)).

(29) Lakowicz, J. R. *Principles of Fluorescence Spectroscopy*, Plenum Press: New York, 1983; p 305.

(30) (a) Oevering, H.; Paddon-Row, M. N.; Heppener, M.; Oliver, A. M.; Cotsaris, E.; Verhoeven, I. W.; Hush, N. S. *J. Am. Chem. Soc.* **1987**, *109*, 3258. (b) Kavarnos, G. J.; Turro, N. J. *Chem. Rev.* **1986**, *86*, 401–449.

(31) Marcus, R. A.; Sutin, N. *Biochim. Biophys. Acta* **1985**, *811*, 265 and references cited therein.

Table V. Calculated Förster Energy Transfer Rates[a]

compd	$k_{FT} \times 10^{-9}$ s^{-1}			
	hexane	acetonitrile	methanol	water
IA	0.016	0.081	0.014	0.150
IIA	0.005	0.004	0.008	0.014
IIIA	0.010	0.009	0.024	0.060
IVA	0.010	0.026	0.025	0.025

[a] k_{FT} calculated from eq 7a by using the average values of R and κ^2 (Table IV) and ϕ_d and τ_d values from Table II; J_F values generated from eq 6a.

Furthermore, equation 7a can be employed to calculate k_{FT} from R and κ^2 values (Table IV); these predicted Förster transfer rates (Table V) are more than an order of magnitude lower than the measured values of k_q. Moreover, choosing a value of $^2/_3$ for κ^2, corresponding to randomized donor–acceptor orientations,[29] increases k_{FT} to a maximum of only ~15% of the observed k_q values. Even in the case of anthracene, where the spectral overlap with TEMPOL is maximal for the family of linear aromatic ring systems, we calculate that the quenching radius for Förster energy transfer extends to only 9 Å (in ethanol).

We conclude that energy transfer through either a Förster or Dexter mechanism cannot account for the observed magnitude and (lack of) variation in the intramolecular quenching rate constants.

2. Electron Transfer. For electron transfer to be operative, the energy of the excited singlet must be sufficient to drive the relevant redox couple.[30,31] In the absence of Coulombic interactions, the thermodynamic driving force, ΔG_∞, is given by[30]

$$\Delta G_\infty = -E_{00} + E_{ox} - E_{red} \quad (8)$$

where E_{00} is the 00-excitation energy of the fluorophore, and E_{ox} and E_{red} are the oxidation potential of the electron donor and the reduction potential of the acceptor, respectively.

Assuming a simple continuum model for solute-solvent interaction, additional terms for the Coulombic attraction between the separated charges, ΔG_{Coul}, and for the free energy of solvation of the ion pair, ΔG_{solv}, must be included. The total change in free energy is then given by[30,31]

$$\Delta G_{ET} = \Delta G_\infty + \Delta G_{Coul} + \Delta G_{solv} \quad (9)$$

$$\Delta G_{Coul} = -e^2/\epsilon R \quad (10a)$$

$$\Delta G_{solv} = \frac{-e^2}{2}\left(\frac{1}{r_d} + \frac{1}{r_a}\right)\left(\frac{1}{\epsilon_{MeCN}} - \frac{1}{\epsilon}\right) \quad (10b)$$

and e is the electron charge, ϵ is the solvent dielectric constant, ϵ_{MeCN} is the dielectric constant of acetonitrile in which the redox potentials were measured, R is the distance between donor and acceptor (Table IV), and r_d and r_a are donor and acceptor radii respectively. Coulombic and solvation adjustments to ΔG_∞ are greatest (up to +0.8 eV) in hexane (ϵ = 1.88) and increase steeply with distance in this solvent. For the polar solvents acetonitrile and water, $\Delta G_{Coul} + \Delta G_{solv} < 0.1$ eV and exhibits little distance dependence.

For IA–IVA, the naphthalene moiety may act as either an electron acceptor or donor resulting in oxidation or reduction, respectively, of the nitroxide; these reactions are shown diagramatically in eqs 11 and 12

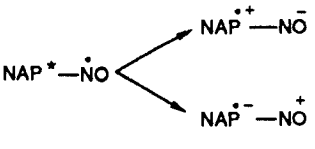

(11) (12)

We calculated ΔG_{ET} for these reactions by employing eqs 8 and 9; results for the most favorable electron transfer route (eq 11 or 12) are given in Table VI. These calculations indicate that in acetonitrile both reduction and oxidation of the nitroxide are thermodynamically feasible but that the oxidative pathway (eq 12) is preferred in all cases by >0.15 eV. In hexane, the lack of solvent stabilization makes reduction of the nitroxide (eq 11) energetically unfavorable and reduces the driving force for the oxidative pathway ($\Delta G_{ET} > -0.4$ eV). In aqueous solution, nitroxide reduction (eq 11) has the greater driving force. Although these calculations suggest that the direction of electron transfer would reverse in water, the quenching rate constants do not differ greatly. If electron transfer is the dominant pathway for quenching, transfer in both directions must be occurring with equal facility.

Table VI. Singlet Energies (E_{00})[a] and Calculated Thermodynamic Driving Forces (ΔG_{ET}) for Electron Transfer[b]

compd	hexane[c,d]		acetonitrile[b]		water[e]	
	E_{00}	ΔG_{ET}	E_{00}	ΔG_{ET}	E_{00}	ΔG_{ET}
IA	3.82	−0.25	3.43	−0.90	3.18	−1.03
ID[f]	3.82	+0.03	3.43	−0.90		
IIA	4.00	+0.07	4.00	−0.87	4.00	−1.85
IIIA	3.72	−0.07	3.65	−1.12	3.30	−1.14
IVA	3.54	−0.29	3.51	−1.33	3.44	−1.28
IVD	3.54	−0.29	3.52	−1.34	–	–

[a] Singlet energies (E_{00}) were obtained experimentally from the intersection points of fluorescence excitation and emission spectra. [b] Calculated from eq 8 in text; units are eV. [c] Favored charge-separated product is (Nap$^-$Nap$^+$). Oxidation potential of TEMPOL (+0.63 V vs SCE) in acetonitrile from ref 2; reduction potentials for 1-,[35] 2-,[35b,c] and 2,6-[35a] substituted naphthoates (−1.92 V, −1.95 V, and −1.55 V, respectively), and 1-methylnaphthalene[35b] (−2.5 V) in dimethylformamide, acetonitrile or 75% dioxane/water were employed to calculate ΔG_∞ for IA, IIIA, IVA, and IIA, respectively. [d] Values in hexane adjusted for solvation (see text) by using eq 10 and the approximation $r_d = r_a$ = 3.8 Å. [e] In water the favored charge-separated product is (Nap$^+$NO$^-$). The reduction of TEMPO gives an irreversible wave in cyclic voltammetry (−0.62 V).[32,33] The oxidation potentials of 1-[35b] and 2-[35b] methyl-naphthalenes (+1.53 and +1.55 V, respectively) in acetic acid solution were used as the best available estimates for potentials of compounds substituted at the 1 and 2-positions. [f] Redox potentials for DOXYL were unavailable; the values for TEMPOL were assumed.

Within individual series of compounds our measured values of k_q do not show any obvious correlation with ΔG_{ET}. For example, the values of k_q for IIA are equal in acetonitrile and hexane, although electron transfer is calculated to be exergonic in the first solvent and endergonic in the latter. Other discrepancies are also apparent. In particular, the k_q's for IIIA and IVA do not vary significantly between acetonitrile and hexane despite the large (~0.8 eV) differences in ΔG_{ET} in these two solvents. Additionally, in polar solvents quenching of IIIA (β-substituted) is slower than IA (α-substituted) by an order of magnitude although its driving force is greater.

Overall, these data are inconsistent with the notion that electron transfer acts as the dominant pathway for singlet quenching.[15a,30,31] The lack of solvent dependence does not, by itself, rule out electron transfer since the rate of transfer is a function of the activation energy, $\Delta G^\ddagger$, which includes an additional solvent dependence in the form of the solvent reorganization energy, λ_S.[30,31] Oevering et al.[30a] have demonstrated that the effect of solvent reorganization on $\Delta G^\ddagger$ may in some cases largely compensate for the solvent dependence included in ΔG_{ET}. We were unable to calculate $\Delta G^\ddagger$ precisely for these compounds owing to uncertainties in sensitive parameters such as the internal (nuclear) reorganization energy and the effective radius of the nitroxide group. Nevertheless, no reasonable values for these parameters lead to a prediction of faster rates in hexane than in acetonitrile as we have observed for several compounds (IA,D). On the basis of these observations, we tentatively conclude that electron transfer does not play a major role in the quenching. The complete lack of radical ion formation during singlet state quenching by nitroxides in polar solvents[1f,g] provides additional support for this view. However, owing to the uncertainties in the simple continuum model and the redox potentials for the nitroxides,[2,32,34] as yet, we are hesitant to exclude

(32) Fish, I. R.; Swarts, S. G.; Sevilla, M. D.; Malinski, T. *J. Phys. Chem.* **1988**, *92*, 3745.
(33) Tsunaga, M.; Iwakura, C.; Tamura, H. *Electrochim. Acta* **1973**, *18*, 241.

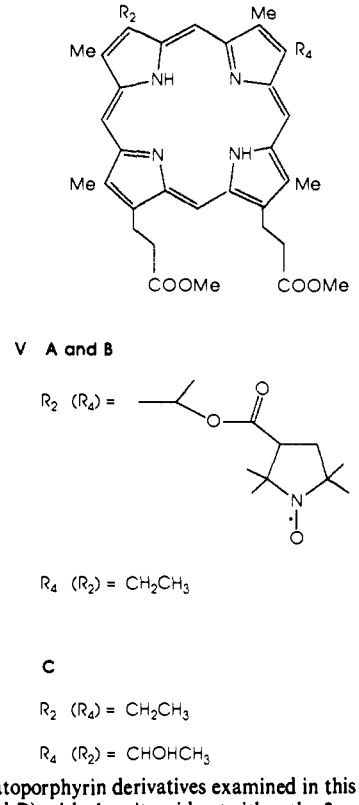

Figure 6. Hematoporphyrin derivatives examined in this study. The two isomers (VA and B) with the nitroxide at either the 2 or 4 position were separated, but were not uniquely identified.

unequivocally a contribution of electron transfer to the quenching.

3. **Electron Exchange.** Electron exchange between the naphthoate singlet and nitroxide doublet can produce rapid relaxation of the excited state.[1,14] Available relaxation routes are as follows:[1] (Dexter) energy transfer (13a), intersystem crossing to triplet (13b), or internal conversion (13c)

$$^2(^1NAP^*—^2NO) \rightarrow \begin{cases} ^2(^1NAP—^2NO^*) & (13a) \\ ^2(^3NAP^*—^2NO) & (13b) \\ \downarrow \\ ^2(^1NAP—^2NO) & (13c) \end{cases}$$

As discussed above Dexter energy transfer is an unlikely relaxation pathway. However, to eliminate energy transfer from consideration and focus on exchange-induced intersystem crossing (13b) or internal conversion (13c), preliminary data were collected on several hematoporphyrin–nitroxide adducts (Figure 6). For these compounds, the energy of the porphyrin singlet (~2.0 eV) is well below that of the pyrrolidinyl nitroxide doublet (~2.9 eV) thus eliminating the possibility of Dexter (or Förster) energy transfer. ΔG_{ET} for these adducts is also calculated to be small (−0.18 eV, nitroxide oxidation).[36] Nevertheless, in methanol, the rate constants for quenching in the A isomer, 6.6×10^8 s^{-1}, and the B isomer, 7.2×10^8 s^{-1}, are comparable to those of IIA. These results suggest that an electron exchange induced intersystem crossing to the triplet or internal conversion to the ground state is occurring.

Further support for an exchange-induced "local" relaxation is provided by the correlation presented in Figure 7. Here we have plotted the k_q's of the paramagnetic compounds against the nonradiative rate constants of their corresponding diamagnetic *O*-acetyl and methyl ester derivatives. With the exception of IVA in methanol, compounds having similar nitroxide–fluorophore distances (e.g. IA, IIA–IVD) exhibit an approximately linear relationship between these parameters. This correlation is interpreted to result from a fixed enhancement (~55-fold) by the nitroxide of a preexisting, nonradiative relaxation pathway in the fluorophore. Because nonradiative decay in most aromatic hydrocarbons proceeds almost exclusively through intersystem crossing (Ermolev's rule[14c]), this enhancement probably reflects a lifting of the spin restriction to singlet–triplet transition brought about through the coupling of the doublet and excited singlet states.[14] We suspect that the relatively minor deviations from this correlation result from variations in the degree of coupling among these derivatives due to small differences in distance, orientation, and structure (Figures 1 and 6).

If intersystem crossing (13b) competes effectively with triplet quenching by the nitroxide (13b → 13c),[3-10] one might expect to see an enhanced phosphorescence signal in nitroxide-substituted compounds as compared with their diamagnetic forms. Observations do not bear this out (Figure 8); triplet (480 nm) and singlet emission bands are both clearly visible for IA, IB, and ID at 77

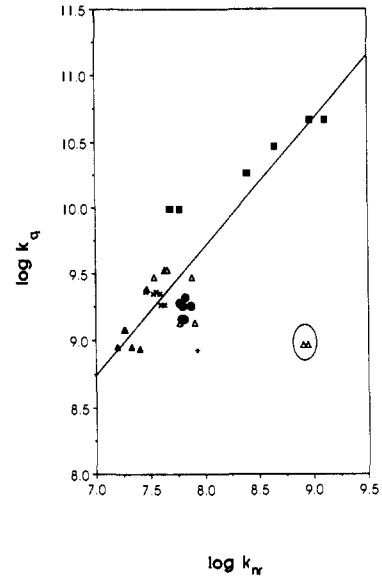

Figure 7. Intramolecular quenching constants (k_q) of nitroxide adducts IA (■), IIA (▲), IIIA (●), IVA (△), IVD (×), and VA (*) vs nonradiative rate constants (k_{nr}) of the corresponding diamagnetic *O*-acetyl and methyl ester derivatives. k_q values for IVD are divided by 2 to account for the presence of two nitroxide groups in this compound. The line represents a linear regression (slope = 0.96, r^2 = 0.76) of all data excluding IVA in methanol (circled) and VA. k_{nr} for VA in methanol was estimated from data of Andreoni et al.[43]

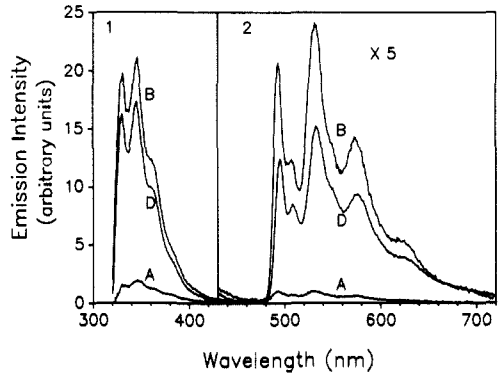

Figure 8. Fluorescence (1) and phosphorescence (2) emission spectra of IA, IB, and ID: excitation wavelength, 300 nm; bandpass, 2 nm; concentration, 15 μM in EPA glass, 77 K. Phosphorescence intensities are expanded by a factor of 5.

(34) While the oxidation potential of TEMPOL exhibits only a slight solvent dependence, its reduction is apparently more favorable by as much as 1 eV in protic solvents, perhaps due to stabilization of the reduced species by protonation (ref 32).

(35) (a) DeLuca, C.; Giomini, C.; Rampazzo, L. *J. Electroanal. Chem. Interfacial Electrochem.* **1986**, *207*, 161. (b) Siegerman, H. In *Technique of Electrorganic Synthesis Part II*; Weinberg, N. L., Ed.; John Wiley and Sons, Inc.: New York, 1975. (c) Klopman, G.; Nasielski, I. *Bull. Soc. Chim. Belg.* **1961**, *70*, 490.

(36) Driving force calculation is based on porphyrin reduction potential of −1.34 V vs SCE (ref 39) and PROXYL oxidation potential of +0.62 V (ref 32). Driving force for porphyrin oxidation/nitroxide reduction is +0.4 V.

K (EPA glass), but for the nitroxide adducts (IA, ID) the triplet emission is diminished to a greater extent than that of the singlet. Thus we cannot distinguish between pathway 13c and a rapid, two-step relaxation via 13b.

Conclusions

For all adducts examined in this study, absorption and fluorescence emission spectral shapes and energies were identical with those of the parent fluorophore. There was no evidence for charge-transfer absorption or charge-recombination emission. We conclude that the emission arises from the same locally excited singlet state in the presence or absence of nitroxide substituents.

Intramolecular quenching of excited singlet states by nitroxyl radicals is very efficient; rate constants are in the range of 10^8–10^{10} s^{-1}. At distances as great as 12 Å, the quenching can occur at rates $> 10^8$ s^{-1}.

Förster energy transfer cannot account for more than a small fraction of the observed rates, even assuming larger values for κ^2. The rates do not show the dependence on overlap integrals predicted by theories of Förster or Dexter energy transfer. There is no clear correlation of k_q values with calculated values of ΔG_{ET}, suggesting that photoinduced electron transfer is also unimportant. Significant quenching rates are obtained in hematoporphyrin–nitroxide adducts which contain a fluorophore whose singlet energy is below that of the lowest excited state of the nitroxide. Since the driving force for electron transfer is also small, this result suggests that the nitroxide moiety facilitates either intersystem crossing to the triplet or internal conversion to the ground state. Further support for exchange-induced relaxation is provided by the linear correlation between k_{nr} and k_q, indicating a fixed enhancement of a preexisting pathway. Thus we conclude that the quenching arises primarily through electron exchange. This conclusion is consistent with earlier studies of diffusional quenching of aromatic hydrocarbons by nitroxides.[1b]

This work provides the first preliminary evidence for long-range quenching by electron exchange *that proceeds via the local relaxation of the singlet and not energy transfer.* That this pathway also appears to out compete or to occur in preference to exergonic electron transfer is somewhat surprising, given current thinking on the relationship between electron-exchange and electron-transfer processes.[15b,30b,42] While compounds containing fluorophores with different structures, singlet energies, and redox potentials could, in principle, exhibit a number of different quenching mechanisms, data from this and previous studies[1] have failed to provide unequivocal evidence for the operation of mechanisms other than electron exchange in the quenching of excited singlet states by nitroxides. Further work employing a series of differing nitroxides and fluorophores combined within a rigid structural framework[15] could provide additional insight concerning the factors controlling the possible relaxation pathways.

Experimental Section

Optical Measurements. Solutions for optical measurements in all solvents were prepared from concentrated (~10 mM) stock solutions in methanol. All solvents were HPLC grade (Aldrich) used without further purification. Absorption spectra were measured on solutions in 1- or 5-cm quartz cells with a Hewlett-Packard 8451A diode array spectrophotometer (spectral resolution, 2 nm).

Quantum yield measurements were made on an SLM-Aminco SP-F-500C spectrofluorometer linked to an IBM PC-XT for data collection and processing. Freshly made solutions had optical densities of ≤0.02 at the excitation wavelength, chosen as the absorbance maximum in the range of 280–300 nm. Excitation and emission bandpasses were 2 nm in most cases; 4-nm bandpasses were used to measure some of the very low quantum yields. Samples were thermostated at 20 °C. Solutions were deoxygenated through bubbling with N_2; emission scans were repeated until bubbling caused no further increase in fluorescence intensity. Any signal due to the solvent was removed by subtraction. Spectra were corrected for instrumental response and integrated by using correction factors and software provided by the manufacturer. (A modified correction procedure was used to avoid arbitrary normalization and conversion steps in the standard routines).

Quantum yields were calculated with respect to quinine sulfate in 0.1 N H_2SO_4 (OD = 0.02) and corrected for refractive index differences between solvents, by using

$$\phi = \frac{F_s A_{qs} \eta s^2 \phi_{qs}}{A_s F_{qs} \eta_0^2} \tag{14}$$

where the subscript s refers to the sample, qs refers to quinine sulfate, ϕ is quantum yield, A is absorbance at the excitation wavelength, F is the integrated, corrected fluorescence, η_s is the refractive index of the sample solvent, and η_0 is the refractive index of water. ϕ_{qs} is 0.55.

Fluorescence lifetimes were measured by time-correlated single-photon counting, on an instrument generously made available through the Laser Biomedical Research Center at MIT. Excitation was provided by a cavity-dumped tunable dye laser, synchronously pumped with the second harmonic of a mode-locked Nd-YAG (Coherent, Antares 76-S). For the naphthalene derivatives the dye pulses (5 ps fwhm, 20 MHz) were frequency doubled with a phase matched KTP crystal to 295 nm. The porphyrin derivatives were excited directly with the dye laser, tuned to 580 nm. Fluorescence from deoxygenated samples was collected at 90° (naphthalene derivatives) or 180° (porphyrin derivatives) and focused into a Spex monochrometer; entrance and exit slits were adjusted to obtain a counting rate of 4000–5000 photons per second impinging on the PMT.

A Canberra 2143 time-amplitude converter (TAC) received start pulses directly from the cavity dumper and stop pulses from the PMT. The TAC signal was passed to a multichannel analyzer and the data were saved in an IBM PC-XT for later analysis with a Sun microcomputer. The instrumental response limit for this system is about 70 ps.

Determination of Minimal-Energy Conformations of IA–IIIA. The general strategy for this search was to allow the functional groups of each compound to freely rotate around all nonconjugated bonds that were not in constrained ring structures. There were two degrees of rotational freedom in IA and IIIA: (1) the bond between the carboxyl carbon and oxygen atoms of the ester linkage; and (2) the carboxyl oxygen and carbon C1 of the nitroxyl ring. The functional groups were rotated through 360° around each of these two bonds in 5° increments. The structures after each rotation were energy-minimized by using AMBER[28] to optimize the bond distances, bond angles, dihedral angles of the bonds, and dipole and van der Waal's interactions. The structures were allowed to minimize to a convergence of 1.0×10^{-1} kcal/mol difference in overall energy, and 0.10 kcal/mol Å in the gradient of the overall energy. An analysis of the energies associated with each rotation versus the angle of rotation around each degree of freedom showed that the local energy wells were greater than ±10° in width relative to the angles of the minimized conformations. Thus a smaller rotational increment was not necessary in searching for the global energy minima.

The addition of a methylene group between the naphthalene ring and the carboxylate introduces two additional degrees of rotational freedom to IIA. To simplify this system, the structure was allowed to energy minimize in terms of only the naphthalene ring and the intervening methylene group. This fixes the methylene hydrogens in orientations that are not sterically hindered by the aromatic ring. The structure was then treated in the same fashion as IA and IIIA through rotations around the two carbon–oxygen bonds in the ester linkage, but also including the additional rotation about the methylene–carboxylate bond.

Preparation of Nitroxide Derivatives. General. All starting materials and reagents were obtained from Aldrich and used as received. High purity grade Burdick and Jackson solvents were used following distillation over CaH_2 in all preparations. Chromatographic separation was obtained on a flash column using 30μm silica (Amicon or Davisil) under positive N_2 pressure; solvents are indicated where appropriate. Melting points, which are uncorrected, were measured on a Mel-temp apparatus (Laboratory Devices). Infrared (IR) spectra were recorded as a thin film on a Mattson Sirrus 100 infrared spectrophotometer at 4 cm^{-1}. Mass

(37) Hassner, A.; Alexanian, V. *Tetrahedron Lett.* **1978**, *46*, 4475–4478.
(38) Smith, K. M., Ed. *Porphyrins and Metalloporphyrins*; Elsevier Scientific Publishing Co.: Amsterdam, 1975.
(39) Felton, R. H. In *The Porphyrins*; Dolphin, D., Ed.; Academic Press: New York, 1978.
(40) Suzuki, S.; Fujii, T.; Ishikawa, T. *J. Mol. Spectrosc.* **1975**, *57*, 490.
(41) Orchin, M.; Jaffe, H. H. *Symmetry, Orbitals and Spectra*; John Wiley and Sons, Inc.: New York, 1971; pp 204–230.
(42) (a) Closs, G. L.; Piotrowiak, P.; MacInnis, J. M.; Flemming, G. R. *J. Am. Chem. Soc.* **1988**, *110*, 2652. (b) Closs, G. L.; Johnson, M. D.; Miller, J. R.; Piotrowiak, P. *J. Am. Chem. Soc.* **1989**, *111*, 3751.
(43) Andreoni, A.; Cubeddu, R.; De Silvestri, S.; Jori, G.; Laporta, P.; Reddi, E. *Z Naturforsch.* **1983**, *38*, 83.

spectra (MS) were obtained by thermal desorption from a copper probe, in either an electron impact (EI) or chemical ionization (CI) mode on a Finnigan 4510 spectrometer interfaced with an INCOS 2300 data system. CI mass spectra of nitroxide derivatives gave an $(M + 2)^+$ molecular ion, suggesting the nitroxide derivative is chemically reduced prior to ionization in the mass spectrometer. This was not observed in the spectra of nitroxides obtained by EI or in the spectra of the nitroxide–acetyl derivatives by CI. Nuclear magnetic resonance (NMR) spectra of the acetyl derivatives were obtained on either a Bruker AM-250 or Varian XL-300 at Massachusetts Institute of Technology and measured in $CDCl_3$.

1-Oxy-2,2,6,6-tetramethylpiperidin-4-yl 1-Naphthoate (1A). 1-Naphthoyl chloride (950 mg) was dissolved in methylene chloride (10 mL). 4-Hydroxyl-TEMPO (860 mg in 2.0 mL of methylene chloride) was added dropwise to the stirred solution. After 20 h this solution was diluted with methylene chloride, washed with water, dried (Na_2SO_4), and evaporated to an orange oil which later crystallized on standing. Column chromatography (Bio-Rad,Bio-Sil A 100–200 mesh) eluting with methylene chloride and recrystallization from methanol afforded the desired product as orange needles: 962 mg; mp 100–102 °C; IR 1713 cm^{-1}; MS (EI) *m/e* 326 (M^+, 18), 155 (100); MS (CI) 328 ($[M + 2H]^+$, 25), 312 (M − 14, 35), 310 (M − 16, 45), 156 (100).

2-(1-Oxy-2,2,6,6-tetramethylpiperidin-4-yl) 6-Hydrogen Naphthalenedicarboxylate (IVA) and 2,6-Bis(1-oxy-2,2,6,6-tetramethylpiperidin-4-yl) Naphthalenedicarboxylate (IVC). 2,6-Naphthalenedicarboxylic acid (3.5 g) was suspended in methylene chloride (100 mL) and pyridine (3.0 mL). Thionyl chloride (3.0 mL) was then added dropwise, and the resultant solution was stirred until no suspension remained and the solution was clear. The intermediate diacid chloride was evaporated to dryness in an effort to remove extraneous thionyl chloride then dissolved in methylene chloride (150 mL) and pyridine (3.0 mL). 4-Hydroxy-TEMPO (1 g) in a small amount of methylene chloride was added and this mixture stirred overnight. Water (3.0 mL) was added and the precipitated diacid was filtered off and washed with excess methylene chloride. The combined filtrate was washed with water, dried with anhydrous sodium sulfate, and evaporated to a dark orange oil. The desired products were separated and purified by flash chromatography (eluting with 3% methanol/methylene chloride) and recrystallized from methanol giving compound IVA (90 mg) and compound IVD (220 mg). Compound IVA: mp >200 °C dec); IR 3200–2200 cm^{-1} (b), 1715, 1622 cm^{-1}; MS (EI) *m/e* 370 (M^+), 199 (80), 124 (100). Compound IVD: mp >225 °C dec; IR 1712 cm^{-1}; MS *m/e* (EI) 524 (M^+, 30), 370 (20), 124 (100).

1-Oxy-2,2,6,6-tetramethylpiperidin-4-yl 2-Naphthoate (IIIA). 2-Naphthoyl chloride (380 mg) and 4-Hydroxy-TEMPO (345 mg) were dissolved in cold pyridine and stirred overnight (20 h). This mixture was diluted with methylene chloride, washed with water (1 × 25 mL) and 1N HCl (3 × 25 mL), dried over anhydrous sodium sulfate, and evaporated to dryness. The desired product was purified by flash chromatography (methylene chloride), obtained as a solid and recrystallized from methylene chloride/*n*-hexane: 235 mg; mp 122–123 °C; IR 1713 cm^{-1}; MS *m/e* 328 ($(M + 2)^+$, 75), 312 (M − 14, 70), 310 (M − 16, 50), 156 (100).

1-Oxy-2,2,6,6-tetramethylpiperidin-4-yl Naphth-1-ylacetate (IIA). 1-Naphthylacetic acid (500 mg) was combined with dicyclohexylcarbodiimide (DCC, 610 mg), (dimethylamino)pyridine (DMAP, 32 mg), and 4-Hydroxy-TEMPO (462 mg) and dissolved in methylene chloride and stirred overnight under an atmosphere of N_2.[37] The solid dicyclohexyl urea was filtered off and further rinsed with methylene chloride. The combined filtrate was washed with 1 N HCl (2 × 75 mL) and water (3 × 75 mL), dried (Na_2SO_4), and evaporated. The product was purified by flash chromatography (methylene chloride) and evaporated to an orange oil which did not crystallize: IR 1733 cm^{-1}; MS (CI) *m/e* 342 ($(M + 2)^+$, 25), 326 (M − 14, 40), 324 (M − 16, 38), 156 (100).

17β-Hydroxy-4′,4′-dimethylspiro(5α-androstane-3,2′-oxazolidin)-3′-yloxy, Naphthoate (ID). Compound ID was prepared by the DCC coupling described above with use of 1-naphthoic acid and 3-DOXYL-17β-hydroxy-5 α-androstane (Aldrich). The desired product was purified by TLC on a 1-mm-thick plate (20 × 20 cm, Whatman) eluted with methylene chloride and obtained as a yellowish solid: mp 153–154 °C; IR 1714 cm^{-1}; MS (EI) *m/e* 530 (M^+, 1), 444 (DOXYL fragment loss, 2), 155 (100).

Preparation of Nitroxide–Acetyl Derivatives. 1-Acetoxy-2,2,6,6-tetramethylpiperidin-4-yl 1-Naphthoate (IB). Compound IA (50 mg) dissolved in tetrahydrofuran (3 mL) in the presence of 5% palladium/carbon (5 mg) was stirred under an atmosphere of hydrogen for 3 h. After this time the solution was filtered directly (with minimal exposure to air) into a solution of acetic anhydride/pyridine (1:10) which had been previously deoxygenated with nitrogen. This solution was stirred for 20 h under N_2 then diluted with methylene chloride, washed with water, dried, and evaporated to a yellowish oil. After chromatography on silica (eluting with methylene chloride) fractions containing product crystallized after solvents were removed. The final product was recrystallized from methanol to remove a small amount of compound IA and gave a snowy white solid: 20 mg; mp 86–87 °C; IR 1712, 1770 cm^{-1}; MS (EI) *m/e* 369 (M^+), 327 (M^+ − 42), 155 (90), 140 (100); NMR (250 MHz) δ 8.80 (d), 8.14 (d), 8.02 (d), 7.88 (d) 7.55 (m) (7 H, 2,3,4,5,6,7,8-H), 5.45 (m, 11-H), 2.13 (s, OCOMe), 2.20–2.00 (m, 4 H, 12-CH_2), 1.35, 1.17 (s, 12 H, 13a-Me).

2-(1-Acetoxy-2,2,6,6-tetramethylpiperidinyl-4-yl) 6-Hydrogen Naphthylenedicarboxylate (IVB), 2,6-Bis(1-acetoxy-2,2,6,6-tetramethylpiperidin-4-yl) Naphthalenedicarboxylate (IVE), 1-Acetoxy-2,2,6,6-tetramethylpiperidin-4-yl 2-Naphthoate (IIIB), and 1-Acetoxy-2,2,6,6-tetramethylpiperidin-4-yl Naphth-1-ylacetate (IIB). These compounds were prepared in a fashion analogous to compound IB. However, the hydroxylamine produced in the catalytic reduction of compound IVA precipitated upon its formation and excess tetrahydrofuran and pyridine was added in order to filter off the catalyst. Compound IVB was not purified chromatographically but was obtained as a white solid from crystallization in methanol. Compound IVB: IR 1769, 1753, 1715 cm^{-1}; MS (EI) *m/e* 413 (M^+), 371 (M^+ − 42), 140 (100); NMR (250 MHz) δ 8.74, 8.61 (s, 1,5-H), 8.22 (d), 8.18 (m, 4 H 3,4,7,8-H), 5.45 (m, 12-H), 2.16 (s, OCOMe), 2.11 (m, 4 H, 13-CH_2), 1.34, 1.18 (s 12 H, 14-Me). Compound IVE: IR 1766, 1703 cm^{-1}; MS (EI) *m/e* 610 (M^+, 5), 568 (M^+ − 42, 30), 124 (100); NMR (250 MHz) δ 8.58 (s, 1,5-H), 8.04 (m, 3,4,7,8-H), 5.43 (m, 12-H), 2.13 (s, OCOMe), 2.03 (m, 4 H, 13-CH_2), 1.33, 1.16 (s, 12 H, 14-Me). Compound IIIB: mp 115–116 °C; IR 1732 cm^{-1}; MS (CI) *m/e* 398 (M + 29, 5), 370 ($(M + 1)^+$, 100), 310 (M − CH_3CO_2H, 95), 198 (30); NMR (250 MHz) δ 8.54 (s, 1 H, 1-H), 8.00 (d), 7.94 (d), 7.86 (d), 7.55 (m) (6 H, 3,4,5,6,7,8-H), 5.39 (m, 11-H), 2.11 (s, OCOMe), 2.15–1.90 (m, 4 H, 12-CH_2), 1.31, 1.14 (s, 12 H, 13a-Me). Compound IIB: IR 1767, 1732 cm^{-1}; MS (CI) *m/e* 412 (M + 29, 5), 384 ($(M + 1)^+$, 100), 324 (M − CH_3CO_2H, 100), 198 (45); NMR (250 MHz) δ 7.96 (d), 7.84 (d), 7.77 (d), 7.49 (m), 7.38 (m) (7 H, 2,3,4,5,6,7-H), 5.06 (m, 11-H), 4.02 (s, 2 H, 1a-CH_2), 2.06 (s, OCOMe), 1.90–1.67 (m, 4 H, 12-CH_2), 1.17, 1.04 (s, 12 H, 13a-Me).

Preparation of Methyl Esters. Methyl 1-Naphthoate (IC) and Methyl 2-Naphthoate (IIIC). 1-Naphthoyl chloride (500 mg) 1 or 2-naphthoyl chloride was dissolved in cold pyridine (3 mL), methanol (2 mL) was added, and the resultant mixture was stirred in an ice bath for 2 h and at room temperature for an additional 4 h after which time the reaction mixture was diluted with methylene chloride, washed with water (1 × 25 mL), 1 M HCl (3 × 25 mL), dried (Na_2SO_4), and evaporated to dryness. The product was purified by flash chromatography (methylene chloride). Compound IC: obtained as a colorless oil; IR 1711 cm^{-1}. Compound IIIC: obtained as a solid and recrystallized from methylene chloride/*n*-hexane; mp 72–73 °C; IR 1711 cm^{-1}; MS (CI) *m/e* 215 ($(M + 29)^+$, 15), 187 ($(M + 1)^+$, 100), 155 (10).

2-Methyl 6-Hydrogen Naphthalenedicarboxylate (IVC), 2,6-Dimethyl Naphthalenedicarboxylate (IVF), and Methyl Naphth-1-ylacetate (IIC). Compounds IVC and F were prepared by the procedure used in the synthesis of compounds IVA and D substituting methanol for 4-Hydroxy-TEMPO. Compound IVC: mp >200 °C dec; IR 1721, 1682 cm^{-1}, MS (CI) *m/e* 259 (M + 29, 15), 231 ($(M + 1)^+$, 100); NMR (250 MHz, $CDCl_3$ and d_5-pyridine) δ 8.69, 8.61 (s, 1,4-H 8.20 (dd), 8.08 (dd),7.98 (d) (4 H, 3, 4,7,8-H), 3.96 (s, 3 H, 2a-OMe). Compound IVF: mp 188 °C (lit.[44] mp 186 °C), IR 1707 cm^{-1}. Compound IIC was prepared by the procedure used for the synthesis of compound IIB substituting methanol for the nitroxide: obtained as a colorless oil; IR 1736 cm^{-1}; MS (CI) *m/e* 229 ($(M + 29)^+$, 8), 201 ($(M + 1)^+$, 100), 169 ($(M + 1)^+$ –OMe, 65).

Preparation of Hematoporphyrin IX Carboxy-PROXYL Derivatives. 2(4)-Vinylhematoporphyrin IX DME was obtained from commercial hematoporphyrin IX (Aldrich) by the H_2SO_4/methanol procedure reported by Smith.[38] The product was purified by flash column on silica (3–5% methanol/methylene chloride) and obtained as a solid from methylene chloride/*n*-hexane. At this point, no effort was made to resolve the isomeric mixture of 2(4)-Vinylhematoporphyrin IX DME.

Vinylhematoporphyrin IX DME: IR 3442 (bd, O–H), 3319 (m, N–H), 1734 (s, ester C=O) cm^{-1}; MS (CI) *m/e* 637 ($(M + 29)^+$, 8), 609 ($(M + 1)^+$, 70), 591 ($(M + 1)^+ - H_2O$, 100); NMR (300 MHz) δ 10.18, 10.06, 10.01, 9.93, 9.91, 9.88 (4 H, a, b, g, and d meso-H), 8.20 (m, 1 H, 2a- and 4a-H of vinyl), 6.35, 6.17 (m, 3 H, 2a- and 4a-H of hydroxyl ethyl and 2b- and 4b-CH_2), 4.31 (4 H, 6a- and 7a-CH_2), 3.65, 3.61, 3.55, 3.53, 3.50, 3.43, 3.42 (overlapping s's, 18 H, 1,3,5,8-Me and 6,7-OMe), 3.23 (t, 4 H, 6b- and 7b-CH_2), 2.12 (d, 3 H, 2a- and 4a-Me).

2(4)-1-(Hydroxyethyl)-4(2)-ethyl-6,7-bis[2-(methoxycarbonyl)-ethyl]-1,3,5,8-tetramethylporphyrin (VC). 2(4)-Vinylhematoporphyrin IX DME dissolved in tetrahydrofuran in the presence of 5% palladi-

(44) Buckingham, J., Ed. *Dictionary of Organic Compounds*; Chapman and Hall: New York, 1982; Vol. 4.

um/carbon (5 mg) was stirred under an atmosphere of hydrogen overnight. After the catalyst was filtered off, the desired product was purified on a flash column (3% methanol/methylene chloride) and obtained as a solid: IR 3454 cm^{-1} (bd, O-H), 3318 (m, N-H), 1735 (s, ester C=O); MS (CI) *m/e* 639 ($(M + 29)^+$, 10), 611 ($(M + 1)^+$, 100), 593 ($(M + 1)^+ - H_2O$, 95); NMR (300 MHz) δ 10.34, 10.03, 10.01, 10.00, 9.99, 9.97 (4 H, a, b, g, and d meso-H), 6.32 (q, 1 H, 2a- and 4a-H of hydroxy ethyl), 4.34 (m, 4 H, 6a- and 7a-CH_2), 4.05 (m, 2 H, 2a- and 4a-CH_2), 3.66, 3.65, 3.64, 3.57, 3.56, 3.55 (overlapping s's, 18 H, 1,3,5,8-Me and 6,7-OMe), 3.25 (t, 4 H, 6b- and 7b-CH_2), 2.14 (d, 3 H, 2a- and 4a-Me of hydroxy ethyl), 1.84 (t, 3 H, 2a- and 4a-Me of ethyl).

2(4)-[1-[[(1-Oxy-2,2,5,5-tetramethylpyrrolidin-3-yl)carbonyl]oxy]-ethyl]-4(2)-ethyl-6,7-bis[2-(methoxycarbonyl)ethyl]-1,3,5,8-tetramethylporphyrin (VA,B). The nitroxide derivative was prepared by the DCC coupling reaction with 3-carboxy-PROXYL and the hydroxy porphyrin. A and B isomers were separated by TLC (3‰ methanol/methylene chloride) but were not uniquely identified as to substituant position (2 or 4). *2(4)-carboxy-PROXYL-4(2)-ethylhematoporphyrin IX DME (VA)*: IR 3316, (m, N-H), 1735 (s, ester C=O) cm^{-1}; MS (CI) *m/e* 807 ($(M + 29)^+$, 1), 779 ($(M + 1)^+$, 3), 764 ($(M + 1)^+ - 15$, 8), 593 ($[M + 1]^+ - H_2O$, 100).

Acknowledgment. This work was supported by the Office of Naval Research under ONR Contract N00014-87-K-007 and Grant N00014-89-J-1260 (N.V.B.), and ONR Contract N00014-88-K-0388 (P.S.H.). Partial support for SG was provided by the Environmental Protection Agency. Fluorescence lifetime measurements were made possible through MIT's Laser Biomedical Research Center, an NIH funded facility at the George R. Harrison Spectroscopy Laboratory. We also thank K. An for help with the lasers and data deconvolution. This is contribution No. 7348 from the Woods Hole Oceanographic Institution.

Supplementary Material Available: A listing of atomic coordinates for low-energy conformations of IA, IIA, and IIIA (8 pages). Ordering information is given on any current masthead page.

Heterolysis and Homolysis Energies for Some Carbon-Oxygen Bonds

Edward M. Arnett,* Kalyani Amarnath, Noel G. Harvey, and Sampath Venimadhavan

Contribution from the Department of Chemistry, Duke University, Durham, North Carolina 27706. *Received March 30, 1990*

Abstract: Methods described previously for obtaining heterolysis (ΔH_{het}) and homolysis (ΔH_{homo}) enthalpies for bonds that can be cleaved to produce resonance-stabilized carbenium ions, anions, and radicals are extended to the study of carbon-oxygen bonds through the reactions of resonance-stabilized carbenium ions with substituted phenoxide ions. Titration calorimetry was used to obtain the heat of heterolysis, and the second-harmonic ac voltammetry (SHACV) method was used to obtain reversible oxidation potentials for the anions. In several cases, the electrode reactions were so fast that reversible potentials were obtained only with the greatest difficulty. Nonetheless, there is remarkably good agreement between these oxidation potentials for phenoxide ions obtained by electrochemical methods in sulfolane solution and those reported by others using entirely different techniques in different media. Such agreement provides unprecedented evidence for the soundness of the various methods used to study redox potentials of organic ions and radicals. As before, a wide variety of correlations was tested between ΔH_{het} and ΔH_{homo}. These two properties showed little correlation with each other, but ΔH_{het} gave good correlations between many properties for which neutral species are converted into ions or vice versa, such as redox potentials of both types of ions, the pK_as of the anions, or the free energies of electron transfer. In contrast to the earlier study of cleavage to carbanions and carbenium ions, the present ΔH_{het} values are predicted well by a general equation that employs the pK_{R+} of the carbenium ion (without modification) and the pK_a of the phenol. The improvement is consistent with the fact that the cleavage of carbon-oxygen bonds of the triarylcarbinols used to establish the pK_{R+} stability scale is a more appropriate model for the heterolysis of carbon-oxygen bonds in sulfolane at 25 °C than it is for the cleavage of carbon-carbon bonds under the same conditions.

Introduction

The present paper is relevant to the general question of the formation and cleavage of carbon-oxygen bonds and to more specialized matters such as the degradation of natural and synthetic polymers. The precursor materials, such as lignin from which coals are formed, contain various types of carbon-oxygen linkages (e.g., O-CH_3).[1-6] Phenols, catechols, and methoxyphenols are present in xylem tissue from degraded wood and coalified logs.[4] Stein has shown recently that the carbon-oxygen bond is one of the first bonds to be homolyzed during depolymerization of coal.[7,8]

Scheme I

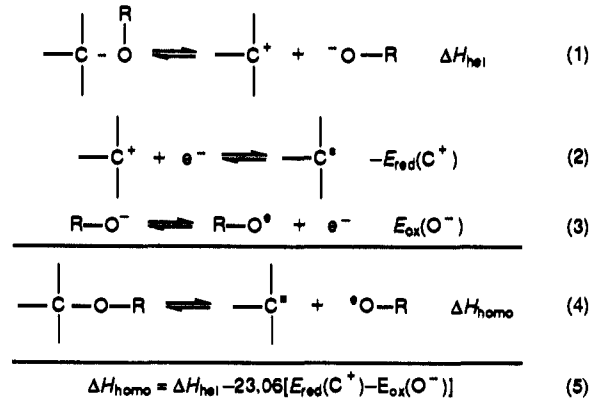

Electron-pair bonds have two possible modes of cleavage: heterolysis to form a pair of ions or homolysis to produce a pair of the corresponding radicals.[9] Since all chemical reactions occur through the making and breaking of bonds, reliable heats of

(1) Farooque, M.; Coughlin, R. W. *Fuel* **1979**, *58*, 705.
(2) Matheson, J. D.; Hansen, L. D.; Eatough, D. J.; Lewis, E. A. *Thermochim. Acta* **1989**, *154*, 145.
(3) Stock, L. M. *Acc. Chem. Res.* **1989**, *22*, 427.
(4) Hatcher, P. G.; Lerch, H. E., III; Kolra, R. K.; Verheyen, T. V. *Fuel* **1988**, *67*, 1069.
(5) Taylor, N.; Gibson, C.; Bartle, K. D.; Mills, D. G.; Richards, D. G. *Fuel* **1985**, *64*, 415.
(6) Hedenburg, J. F.; Freiser, H. *Anal. Chem.* **1953**, *25*(9), 1355.
(7) Suryan, M. M.; Kafafi, S. A.; Stein, S. E. *J. Am. Chem. Soc.* **1989**, *111*, 1423.
(8) Suryan, M. M.; Kafafi, S. A.; Stein, S. E. *J. Am. Chem. Soc.* **1989**, *111*, 4594.
(9) Ingold, C. K. *Structure and Mechanism in Organic Chemistry*, 2nd ed.; Cornell University Press: Ithaca, 1969; pp 5 and 6.

0002-7863/90/1512-7346$02.50/0